

RADIO DETECTION OF A CANDIDATE NEUTRON STAR ASSOCIATED WITH GALACTIC CENTER SUPERNOVA REMNANT SAGITTARIUS A EAST

JUN-HUI ZHAO¹, MARK R. MORRIS² & W. M. GOSS³

¹Harvard-Smithsonian Center for Astrophysics, 60 Garden Street, MS 78, Cambridge, MA 02138
jzhao@cfa.harvard.edu

²Department of Physics and Astronomy, University of California, Los Angeles, CA 90095
morris@astro.ucla.edu

³NRAO, P.O. Box O, Socorro, NM 87801, USA
mgoss@aoc.nrao.edu

Draft: September 23, 2013

ABSTRACT

We report the VLA detection of the radio counterpart of the X-ray object referred to as the ‘‘Cannonball’’, which has been proposed to be the remnant neutron star resulting from the creation of the Galactic Center supernova remnant, Sagittarius A East. The radio object was detected both in our new VLA image from observations in 2012 at 5.5 GHz and in archival VLA images from observations in 1987 at 4.75 GHz and in the period from 1990 to 2002 at 8.31 GHz. The radio morphology of this object is characterized as a compact, partially resolved point source located at the northern tip of a radio ‘‘tongue’’ similar to the X-ray structure observed by Chandra. Behind the Cannonball, a radio counterpart to the X-ray plume is observed. This object consists of a broad radio plume with a size of $30'' \times 15''$, followed by a linear tail having a length of $30''$. The compact head and broad plume sources appear to have relatively flat spectra ($\propto \nu^\alpha$) with mean values of $\alpha = -0.44 \pm 0.08$ and -0.10 ± 0.02 , respectively; and the linear tail shows a steep spectrum with the mean value of -1.94 ± 0.05 . The total radio luminosity integrated from these components is $\sim 8 \times 10^{33}$ erg s⁻¹, while the emission from the head and tongue amounts for only $\sim 1.5 \times 10^{31}$ erg s⁻¹. Based on the images obtained from the two epochs’ observations at 5 GHz, we infer the proper motion of the object: $\mu_\alpha = 0.001 \pm 0.003$ arcsec yr⁻¹ and $\mu_\delta = 0.013 \pm 0.003$ arcsec yr⁻¹. With an implied velocity of 500 km s⁻¹, a plausible model can be constructed in which a runaway neutron star surrounded by a pulsar wind nebula was created in the event that produced Sgr A East. The inferred age of this object, assuming that its origin coincides with the center of Sgr A East, is approximately 9000 years.

Subject headings: Galaxy:center — ISM:individual (Sagittarius A) — ISM: supernova remnant — ISM: radio continuum — stars: neutron; stars: winds, outflow

1. INTRODUCTION

Using X-ray data observed with the Chandra observatory, Park et al. (2005) found a hard compact X-ray source, CXOG J174545.5-285829, having unusual X-ray characteristics compared to most other X-ray sources near the Galactic center. The authors suggested that the X-ray object could be identified as a high-velocity neutron star, produced from the core-collapse supernova (SN) explosion that created the Galactic center supernova remnant (SNR), Sagittarius A East. The X-ray data appear to be consistent with previous radio studies in which Sgr A East was interpreted simply as a supernova remnant (SNR) (Jones 1974; Green 1984; Goss et al. 1985). However, because of the closeness to the supermassive black hole (SMBH), the inferred large energy budget ($\sim 10^{52-53}$ erg), and the elongated morphology and size, alternative ideas have been proposed to interpret the nature of Sgr A East. For example, multiple SN explosions, tidal disruption of a star by the SMBH, or a hypernova associated with a collapsar or microquasar have been suggested (Yusef-Zadeh & Morris 1987a; Mezger et al. 1989; Khokhlov & Melia 1996; Lee et al. 2007). Based on a comprehensive analysis of X-ray data, Maeda et al. (2002) concluded that Sgr A East originated from a single Type II SN explosion and can be classified as a metal-rich ‘‘mixed morphology’’ SNR formed $\sim 10,000$ years ago. The age of Sgr A East inferred from the various models spans a large range, from 1700 yr to 5×10^4 yr. The younger age is associated with a large projected radial expansion velocity of $\sim 2.3 \times 10^3$ km s⁻¹, as described by Rockefeller et al. (2005) who simulated a SN explosion in the Galactic center environment. The oldest age is based on a large input energy of $\sim 4 \times 10^{52}$ erg (corresponding to the

simultaneous explosion of ~ 40 SNe) required to expand into a giant molecular cloud of density $\sim 10^4$ cm⁻³, as indicated in the observations of dust and molecular gas (Mezger et al. 1989; Mezger, Duschl, & Zylka 1996); an expansion velocity of only about 70–80 km s⁻¹ is inferred for this scenario.

2. OBSERVATIONS & DATA REDUCTION

2.1. 5 GHz data

The 2012 epoch data were obtained from our most recent observations of Sgr A that were carried out at 5 GHz in the spring (March 29 and April 22) and summer (July 24 and 27) of 2012 using the Jansky Very Large Array (VLA) in the C and B array configurations, respectively, with total bandwidth of 2 GHz. The UT dates were used throughout the paper. The observations were carried out in spectral line mode with a channel width of 2 MHz for each of 1024 channels so that the frequency-dependent effects in the broadband synthesis imaging can be determined and addressed. The final images have been corrected for frequency-dependent effects. The detailed process of data reduction (data editing, calibration and imaging) was performed using the software package of the Common Astronomy Software Applications (CASA) of the National Radio Astronomy Observatory (NRAO). Details will be provided in a subsequent paper (Zhao, Morris & Goss 2013). The final image was constructed using multiple-scale (MS) and multiple-frequency-synthesis (MFS) techniques with robustness weighting parameter of -2 , achieving an rms noise level of $10 \mu\text{Jy beam}^{-1}$ at the phase center with no emission (as reported in Table 1). At the Cannonball, the rms noise in the primary beam (PB) corrected image is $11.4 \mu\text{Jy beam}^{-1}$. The resulting synthesized

full-width-half-maximum (FWHM) beam is $1.6'' \times 0.6''$ (PA= 12°), equivalent to that from uniform weighting.

The B-array data observed on July 24 and 27, 2012 were used to show the structure of compact radio emission associated with the Cannonball. The MS-MFS imaging process was carried out in CASA by fitting the 2-GHz spectra with a Taylor expansion for the first two terms in order to determine the Stokes I and spectral index from 4.4 to 6.4 GHz. The intensity α -image at the reference frequency of 5.5 GHz was derived from the zero-order of the Taylor approximation while the spectral index α -image (α for ν^α) was derived from the second term (tt1) in the first-order of the Taylor approximation. An rms noise level of $15 \mu\text{Jy beam}^{-1}$ is inferred for the radio intensity image from B-array data with a FWHM beam of $1.6'' \times 0.6''$ (10°). At the Cannonball, the rms noise increases to $17 \mu\text{Jy beam}^{-1}$ in the primary-beam-corrected image.

We note that the α -images are subject to large fluctuations propagated from the residual sidelobes in the tt1-image due to imperfect uv-coverage. For the sources with a large S/N (≥ 100) within the half-power beamwidth (HPBW) of the primary beam, the mean value of spectral index from the α -image is reliable (Rau V. Urvashi 2013, personal communication). This statement appears to be consistent with our α -images; towards the regions with S/N in the range from a few hundreds to a few thousands, such as the HII mini-spiral arms of Sgr A West and the HII regions (A -D) located east of Sgr A East, flat and/or gently-rising continuum spectra with less significant fluctuations are in good agreement with the previous spectral image trends derived from 6 and 20 cm VLA data (Pedlar et al. 1989). However, the Cannonball components, with typical S/N ~ 50 , exhibit significant fluctuations in the α -image. Therefore, we only report the mean values of spectral index and cite errors from the standard deviation of the mean on the Cannonball sources (Table 2).

The 1987 epoch data used in this study are from the VLA observations of Sgr A at three reference frequencies, 4.585, 4.815, and 4.915 GHz, in the B array configuration in a spectral line mode with channel width of 3.125 MHz for each of 15 channels. We calibrated the data in AIPS following the VLA standard calibration procedure for a spectral line data set. The radio source 3C 84 was used for calibration of the bandpass, 3C286 for the flux density scale and NRAO 530 for the complex gains. The coordinates of equinox B1950 in the archived data were converted to J2000 using the AIPS task UVFIX. The spectral data were further reduced and binned to 3 channels in CASA for imaging with the MS-MFS technique; thus, with a channel width of 15.6 MHz, the intensity loss due to the effect of the delay beam is negligible. An rms noise level of $130 \mu\text{Jy beam}^{-1}$ was achieved in the final image. At the Cannonball, the rms noise increases to $150 \mu\text{Jy beam}^{-1}$ in the primary beam corrected image.

2.2. 8.3 GHz data

An image was made from the VLA data observed at 8.31 GHz in BnA, CnB and D configurations in nine observations during the period between 1990 July 2 and 2002 May 22. All the observations were carried out in spectral line mode with a channel width of 0.3906 MHz for 31 channels. The data were calibrated in AIPS (see Zhao et al. (2009) for the details of data reduction). The mean observing epoch of the 8.31 GHz data is 1995.9, which is hereafter referred as **the 1995 epoch**. The image was made in CASA using robust=1 weighting with the MFS technique at a center frequency of 8.31 GHz; the synthesized

image was further cleaned with the MS technique. The rms of $35 \mu\text{Jy beam}^{-1}$ was achieved with a FWHM synthesized beam of $0.7'' \times 0.5''$ (PA= 69°). At the Cannonball, the rms is $52 \mu\text{Jy beam}^{-1}$ in the primary-beam-corrected image. The image used in this paper was convolved to a beam of $1.6'' \times 0.6''$ (PA= 10°) to match the beam of the 5.5 GHz image in order to facilitate comparisons between the images from different frequency bands and different time epochs. The parameters of the final images used in this paper are summarized in Table 1.

3. RESULTS

3.1. Detection of a radio counterpart of the X-ray Cannonball

Figure 1 shows the 2012 VLA 5.5 GHz image of the radio emission from Sgr A East. At the tip of a radio emission plume located at the northernmost edge of the Sgr A East shell, a compact radio source was detected coinciding with the X-ray source J174545.5-285828 (Muno et al. 2009)¹. The compact radio source corresponding to the X-ray object was also detected at the northern tip of the radio plume in both the 1987 and 1995 epochs at 4.75 and 8.31 GHz.

Figure 2 shows a comparison between the radio and X-ray sources in the central $5' \times 3.5'$ region of the Galaxy by overlaying the VLA B-array image at 5 GHz on the three-color image made from Chandra observations (Park et al. 2005). The alignment of coordinate frames of the radio and X-ray images was made using the radio counterparts of fourteen compact X-ray sources with positions given in the catalog of Chandra X-ray point sources (Muno et al. 2009). Except for the well-known source Sgr A*, the Cannonball and a dozen additional sources have been newly identified with either compact or filamentary radio sources² which will be discussed in a subsequent paper (Morris et al. 2013). The mean magnitude of the positional offset between the radio and X-ray sources is $1.1'' \pm 0.5''$, which is much greater than the positional offset ($0.24''$) of the Cannonball between the radio (this paper) and the X-ray (Muno et al. 2009). The X-ray position of Sgr A* (Muno et al. 2009) is offset by $0.16''$ from the radio position determined by Reid & Brunthaler (2004). Thus, limited by the uncertainty of the X-ray position for the reference source Sgr A*, the uncertainty in the alignment between radio and X-ray frames (or the rms residual errors) is about $0.2''$. We note that a large fraction of the radio counterparts of the compact X-ray sources are radio filaments; the relatively large positional uncertainties of the linear radio sources result from their confinement in only one dimension, so they are the dominant contribution to the mean positional offset.

In general, the radio emission defining the Sgr A East radio

¹ The X-ray source was originally referred as CXOUGC J174545.5-285829 by Park et al. (2005) based on the position in Muno et al. (2003).

² A list of radio sources (this paper) identified with X-ray point sources (Muno et al. 2009) was used for the alignment of the radio and X-ray coordinate frames (Figure 2):

Id	Radio - RA, Decl. (J2000)	X-ray ID
1.	17 : 45 : 33.610, -29 : 01 : 40.87	CXOUGC J174533.5-290140
2.	17 : 45 : 36.907, -29 : 00 : 39.28	CXOUGC J174536.9-290039
3.	17 : 45 : 37.934, -28 : 59 : 10.03	CXOUGC J174538.0-285911
4.	17 : 45 : 39.294, -29 : 02 : 25.85	CXOUGC J174539.3-290232
5.	17 : 45 : 41.788, -28 : 58 : 16.13	CXOUGC J174541.5-285814
6.	17 : 45 : 41.629, -28 : 59 : 34.00	CXOUGC J174541.6-285934
7.	17 : 45 : 42.269, -28 : 59 : 59.99	CXOUGC J174542.2-285959
8.	17 : 45 : 43.444, -29 : 02 : 14.48	CXOUGC J174543.4-290214
9.	17 : 45 : 44.176, -28 : 59 : 41.17	CXOUGC J174544.1-285940
10.	17 : 45 : 45.883, -28 : 58 : 49.72	CXOUGC J174545.9-285849
11.	17 : 45 : 46.192, -29 : 00 : 56.24	CXOUGC J174546.1-290057
12.	17 : 45 : 46.309, -28 : 57 : 56.17	CXOUGC J174546.2-285756

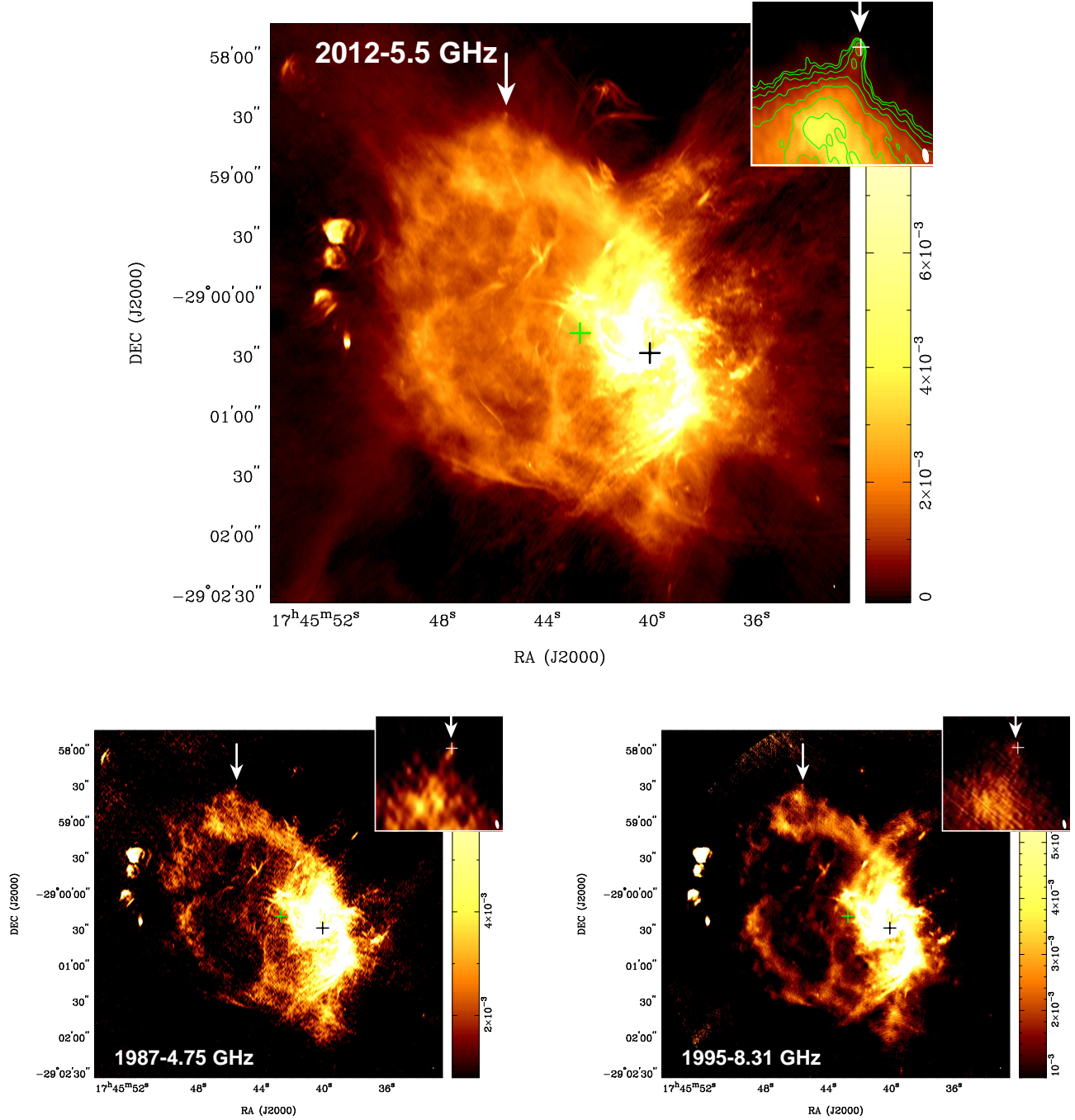


FIG. 1.— The VLA images of Sgr A East, Top: 2012 epoch image at 5.50 GHz constructed with the B and C array data, bottom-right: 1995 image at 8.31 GHz, bottom-left: image made from 1987 data at 4.75 GHz. Sgr A* is marked as a black dot with a superimposed cross located at the center of Sgr A West. The green cross marks the pointing center of the 2012 observations at 5.50 GHz, which is close to the geometrical center of the Sgr A East shell. The radio counterpart of the X-ray object “Cannonball” was detected in all the images, as indicated by a white arrow. The inset at the top right of each image shows a $22'' \times 20''$ region surrounding the Cannonball. The color wedge to the right indicates the radio intensity scale in units of Jy beam^{-1} . Note that the 4.75 GHz image is deconvolved to the common resolution ($1.6'' \times 0.6''$, $\text{PA}=10^\circ$) which is smaller than the synthesized beam of the 4.75 GHz data. The FWHM beam (convolved to $1.6'' \times 0.6''$, $\text{PA}=10^\circ$) is marked at the bottom-right corner. All these images have been corrected for primary beam attenuation.

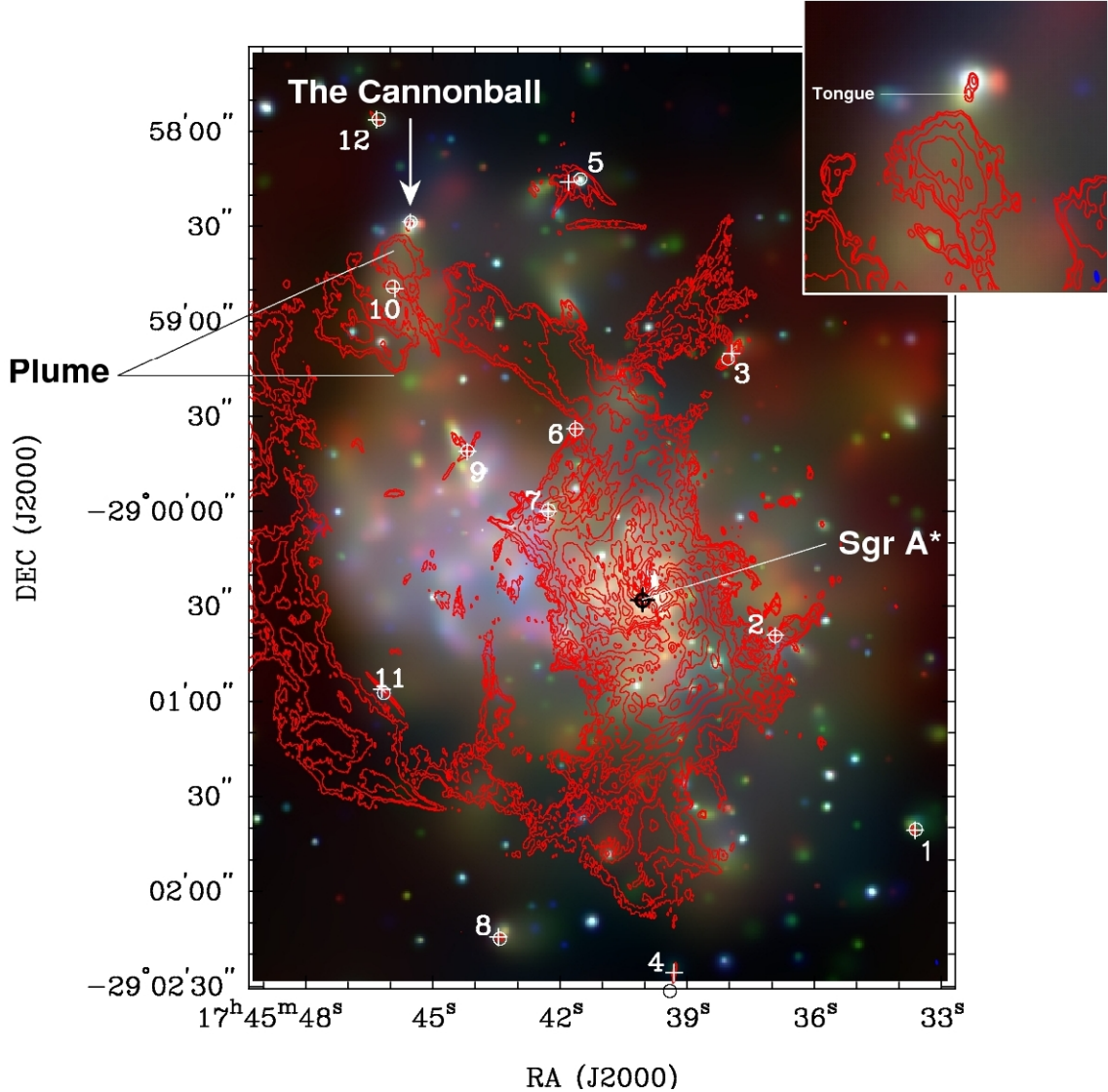


FIG. 2.— The VLA B-array image at 5 GHz (red contours) is overlaid on the Chandra three-color image of the X-ray object “Cannonball” (red represents the 1.5–4.5 keV band photons, green represents 4.5–6.0 keV, and blue represents the 6.0–8.0 keV band) (Park et al. 2005). The radio counterpart of the Cannonball is denoted by the white arrow. The X-ray plume described by Park et al. (2005) is indicated. The black plus symbol marks the radio position of Sgr A*; the black open circle is the X-ray position of Sgr A* (Muno et al. 2009). The rest of the compact and filament radio sources (crosses) identified with X-ray point sources from Muno et al. (2009) (open circles) were used for the alignment between the X-ray and radio frames. The inset at the top-right shows an enlarged image of the area ($\sim 40''$) surrounding the Cannonball.

shell appears to be the extended radio emission that lies just outside the northern, eastern, and southern boundaries of the X-ray emitting region of the mixed-morphology SNR (Maeda et al. 2002). The western boundary appears to overlap with Sgr A West, the mini-spiral of the central HII region and the circumnuclear disk (CND) around the SMBH located at Sgr A*.

The Cannonball is characterized in X-ray images as a high-intensity point source (head) located at the tip of an X-ray plume that appears to point toward the north-northwest, showing a tail extending to the south-southwest (See Figure 2). In addition, a brighter X-ray extension ($5''$) located immediately southeast of the Cannonball head is evident (see the inset of Figure 2). A similar extended structure was also seen in the X-ray image of the Mouse PWN and referred to as a “tongue” (Gaensler et al. 2004). The Mouse is a prototypical PWN; we find that the Cannonball is comparable to the Mouse (see below). We have adopted the nomenclature as described by Gaensler et al.

(2004) to describe the feature of the secondary radio peak associated with the Cannonball head.

Similar to the X-ray morphology, the radio image also shows a compact head slightly resolved in the north-south direction, connected with a plume embedded in the strong radio emission from the northern edge of the Sgr A East radio shell (Figure 1a). In the B-array image (Figures 2 and 3a), the compact portion of the radio plume is shown with enhanced contrast against the extended emission from the region near the northern boundary of Sgr A East, which is closely associated with the X-ray plume.

3.2. Morphology and properties of the radio source

Figure 3 shows an image of radio emission in the $1'$ region near the Cannonball source. The morphology of the radio emission can be characterized as (1) a compact point source at the northern tip of a radio plume, (2) a broad radio plume, and (3) a long linear radio emission tail, passing through a circular cavity in the radio emission:

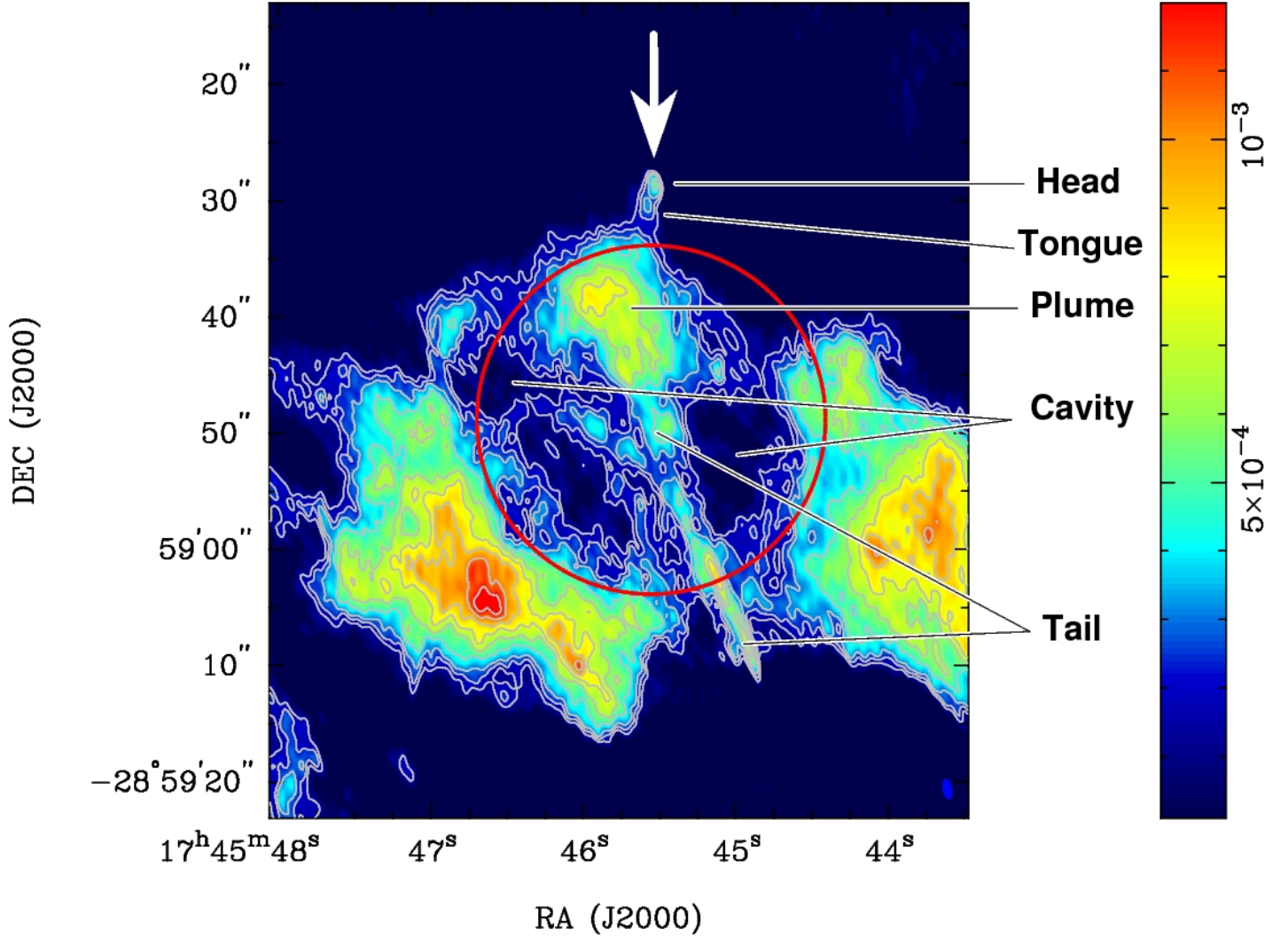


FIG. 3.— The 2012 VLA B-array image of intensity at 5.5 GHz, obtained from the first term Taylor expansion, shows the radio counterpart (indicated by a white arrow) of the X-ray ‘Cannonball’. The color wedge scales the radio intensity in units of Jy beam^{-1} with the FWHM beam ($1.6'' \times 0.6''$, $\text{PA}=10^\circ$) shown at the bottom-right corner. The contours are $15 \mu\text{Jy beam}^{-1} \times (10, 15, 20, 30, 40, 50, 60, 70 \text{ and } 80)$. The red circle marks the cavity region.

TABLE 1
IMAGE LOG

(1)	(2)	(3)	(4)	(5)	(6)
Epoch	ν_c (GHz)	$\Delta\nu$ (GHz)	$\text{Maj} \times \text{Min}$ (PA)	r.m.s. ($\mu\text{Jy beam}^{-1}$)	Array
2012	5.50	2.01	$1.6'' \times 0.6''$ (12°)	10	B & C
2012	5.50	2.01	$1.6'' \times 0.6''$ (10°)	15	B
1995	8.31	0.0004	$0.7'' \times 0.5''$ (69°)	35	Ref.
1987	4.75	0.05	$2.0'' \times 1.0''$ (3°)	130	B

(1) Mean epoch of the images. (2) The center frequencies used in MFS.

(3) The bandwidth of the data. (4) The synthesized beams.

(5) The rms noise level. (6) The array configurations.

Ref: The 8.31 GHz data were summarized in Zhao et al. (2009).

The head of the radio plume can be identified as a marginally resolved compact source that can be fit with a 2D Gaussian having major and minor axes of $2''.0 \pm 0''.2$ and $1''.1 \pm 0''.1$ ($\text{PA} = 170^\circ \pm 5^\circ$). The result from Gaussian fitting shows an elongated structure ($\sim 5''$) in the northwest-southeast direction hereafter referred to as the radio “**tongue**” followed by the radio plume located $5''$, farther south of the compact head. A secondary radio peak is clearly detected $\sim 2''$ southeast of the primary peak of the head in the 2012 image (see Figures 3 and 4). The X-ray image shows a similar structure, a few arcseconds to the southeast of the Cannonball (see Figure 2). The flux density (excluding the secondary peak) of the Cannonball head is $2.0 \pm 0.1 \text{ mJy}$ with a 5.5-GHz peak of $0.51 \pm 0.03 \text{ mJy beam}^{-1}$. The flux density is doubled if including the extended emission from the tongue ($4.1 \pm 0.2 \text{ mJy}$). Along with the values of the flux density and peak intensity derived at 4.75 and 8.31 GHz, we fitted the spectrum and derived the spectral index $\alpha = -0.4$ for the head source, which agrees with the values of the α image derived from the second term of Taylor expansion in the MS-MFS clean of the broadband data at 5.5 GHz

The radio plume is located $\sim 15''$ south-east of the compact source (head), and it can be roughly characterized by an ellipse ($30'' \times 15''$, PA= 80°), embedded in a broad fan-shaped structure as delineated by the northern front of the radio emission. The northern tip of the radio plume is connected with the radio extension (“tongue”) of the head component. A total flux density of 750 ± 150 mJy is estimated for the radio plume. The large uncertainty stems from the uncertainties in defining the boundary, as well as from the determination of the foreground/background emission from the Sgr A East shell. The spectral index of this region appears to have a large error, fluctuating in a range from -1 to 1 . The mean value derived from the α image (Figure 3) is -0.10 ± 0.02 , indicating a rather flat spectrum.

The linear tail extends to the SSW from the plume, approximately pointing to the geometric center of the Sgr A East shell (see the overall image of Sgr A East at 5.5 GHz in Figure 1). The length of this feature is $\sim 30''$ (1.2 pc), with PA= 22° , slightly resolved (deconvolved size of $2''$) in the perpendicular direction. The flux density from this linear feature is 150 ± 40 mJy, peaking near the southern edge of the emission cavity, where a noticeable **notch** is present (Figure 3). Along this linear feature, the spectral index decreases from the peak of the plume, toward the south, so that the steepest spectral slopes are found closest to the center of Sgr A East. We infer a mean value of $\alpha = -1.94 \pm 0.05$ for the tail by averaging the spectral index along it, showing that the spectrum of the tail is rather steep in comparison to other components.

The emission cavity, with a nearly circular shape and a diameter of $30''$, appears to be centered at $\alpha_{J2000} = 17:45:45.6$, $\delta_{J2000} = -28:58:50$. The linear emission tail appears to pass through the low-intensity “notch” located at the southwestern edge of the cavity. The peak of the radio plume lies at the northern edge of the cavity. We note that from the direction of the linear tail (northeastward), the radio head-tongue extension (nearly north) deflects $\sim 25^\circ$ while the Cannonball travelled through the cavity. The X-ray emission shows a similar curvature between the head-tongue and the plume. The radio properties are summarized in Table 2.

3.3. Proper motion

The radio counterpart of the X-ray object was detected from new VLA observations in 2012 at 5.50 GHz and archival VLA observations at both 8.31 and 4.75 GHz. The largest time span between the observations is 25 years. In particular, the B-array observation at 4.75 GHz shows a significant detection ($> 4\sigma$) of the compact radio source corresponding to the Cannonball with a similar uv-coverage as that of the B-array data from the most recent epoch (2012). The new 5.5 GHz observations were centered at the geometrical center of Sgr A East while both the 4.75 and 8.31 GHz observations were at the position of Sgr A*. For all epochs, the offsets ($\Delta\alpha$ and $\Delta\delta$) of the radio object with respect to Sgr A* are given in Table 2. Therefore, the apparent proper motions due to Galactic rotation and Earth’s orbital motion cancel out. We first made a linear regression for the positional offsets of both $\Delta\alpha$ and $\Delta\delta$ including all the three epochs’ data, weighted by the uncertainties ($1/\sigma^2$), with respect to the observing-epoch time to derive the slope using the method and subroutines described in Bevington & Robinson (2002). For $\Delta\delta$, the linear fit gives a correlation coefficient of 0.999 with a probability of no correlation $P_{nc} = 3\%$, while the fit to $\Delta\alpha$ gives a large value $P_{nc} = 90\%$; the regression analysis suggested a significant linear change in $\Delta\delta$ but fluctuations in $\Delta\alpha$ were consistent with noise. We note that errors for the po-

sition of the Cannonball source at the 1995 epoch were large due to the S/N drop for the primary beam attenuation and the poor image fidelity at the source in the 8.31 GHz image. Also, the 1995-epoch image was made from several datasets observed in the period between 1990 and 2002, so the spread in time is quite large compared to that of other epoch images. Therefore, excluding the 8.31 GHz data in our final proper motion fit, we calculate the slopes only from the 6-cm data in the 1987 and 2012 epochs. The linear-fitting plots are given in Figure 4. From the calculated slopes, values of $\mu_\alpha = 0.001 \pm 0.003$ arcsec yr $^{-1}$ and $\mu_\delta = 0.013 \pm 0.003$ arcsec yr $^{-1}$ were inferred for the proper motion of the Cannonball.

We regridded both the 2012 and 1987 images to a common reference frame (the 8.3 GHz reference frame) in order to show the displacement of the radio object by superimposing the two images. We adopted the well-determined position (Reid & Brunthaler 2004) for Sgr A* in the 8.3 GHz reference frame. Figure 4 presents the 2012 image at 5.5 GHz overlaid on top of the 1987 image at 4.75 GHz showing that the radio object has moved northward from the center of Sgr A East (Figure 4). The magnitude of the proper motion is 0.013 ± 0.003 arcsec yr $^{-1}$. At the Galactic center, this proper motion implies a transverse velocity of 500 ± 100 km s $^{-1}$. Such a velocity is comparable to the space velocity of ~ 600 km s $^{-1}$ estimated for the Mouse, a pulsar wind nebula located about a degree away (Gaensler et al. 2004), southeast of the Cannonball.

4. DISCUSSION

4.1. Physical conditions & nature of the Cannonball

The transverse velocity of 500 km s $^{-1}$ inferred from the proper motion of the compact radio source at the head of the Cannonball appears to be consistent with the typical magnitude of a random space velocity that a pulsar may have as a result of the asymmetry in the SN explosion (Chatterjee & Cordes 2002; Gaensler & Slane 2006; Zeiger et al. 2008). Integrating over a frequency range between 0.1 and 100 GHz, assuming a power-law spectrum with the flux density at 5.5 GHz and the spectral index given in Table 2 for each component, we estimate the radio luminosities of the Head, Plume and Tail (Table 3). The luminosity of the radio emission of the Head and Tongue amounts for 1.5×10^{31} erg s $^{-1}$. The total radio luminosity of all three of these components is $L_R \approx 8 \times 10^{33}$ erg s $^{-1}$, which is a typical value for PWN sources. The inferred L_R appears to have the same order of magnitude as the X-ray luminosity (L_X) estimated from Chandra observations (Park et al. 2005). The flat spectrum of the radio emission from the plume ($\alpha = -0.10$) appears to fall in the typical range of $\alpha = 0$ to -0.5 of PWN sources (Gaensler & Slane 2006). Converting the X-ray photon index of $\Gamma = 1.6$ (Park et al. 2005) to α ($\Gamma = 1 - \alpha$), the Cannonball spectral index $\alpha_X = -0.6$ shows that the X-ray spectrum steepens by $\Delta\alpha = 0.5$, a canonical value expected from the aging of synchrotron particles (Woltjer et al. 1997). The radio properties of the Cannonball indicate that the emission is nonthermal synchrotron powered by the energy dissipation of a spin-down pulsar.

The morphology of the radio source associated with the Cannonball shows a compact head with a trailing “tongue” connecting to a broad radio plume followed by a long, linear tail (see Fig. 3). The radio structure of the PWN revealed for the Cannonball is quite similar to that of the Mouse, which has been well studied and modeled. Using the numerical simulations for the Mouse (Gaensler et al. 2004), we have attempted an expla-

TABLE 2
RADIO PROPERTIES OF THE CANNONBALL OBJECT

Epoch [†]	ν_c (GHz)	S_{pk}^\ddagger (mJy b ⁻¹)	S_{tot}^\ddagger (mJy)	α	$\theta_{maj} \times \theta_{min}$ (PA) ("×") (°)	$\Delta\alpha^*$ (^s)	$\Delta\delta^*$ (^{''})
Head:							
2012.567	5.50	0.51±0.03	2.0±0.10	-0.44 ± 0.08	2.0±0.2 × 1.1 ± 0.1(170±5)	5.488±0.001	119.39±0.03
1995.893	8.31	0.42±0.05	1.8±0.30	...	2.9±0.6 × 1.9 ± 0.4(1±14)	5.552±0.015	119.13±0.25
1987.910	4.75	0.8±0.3	2.5±0.4	...	2.6±0.5 × 0.6 ± 0.4(159±10)	5.479±0.005	119.08±0.07
Plume:							
2012.567	5.50	...	750±150	-0.10 ± 0.02	~ 30 × 15 (~ 80)	~5.9	~110
Linear tail:							
2012.567	5.50	...	150±40	-1.94 ± 0.05	~ 30×2 (~22)	~5.1	~86

[†]The observing epochs listed here are the average of the observing dates at each of the frequency bands.

[‡]Peak intensity (S_{pk}) with the FWHM beam = $1.6'' \times 0.6''$ (PA=10°); total flux density (S_{tot}) from the corresponding source area. The flux densities of the Head do not include that of the Tongue. At the epoch of 2012.576, the total flux density of both the Head and Tongue at 5.5 GHz is 4.1 ± 0.2 mJy.

The reference position is Sgr A $\alpha_{J2000} = 17^h45^m40^s.0409$, $\delta_{J2000} = -29^\circ00'28.118''$ (Reid & Brunthaler 2004)

nation of the observed radio components in the context of the shock structure associated with a PWN. Both the compact head with the elongated “tongue” observed in the radio and X-ray indicate the presence of a bow shock caused by the supersonic motion of the pulsar through the ISM. The bow shock confines the pulsar wind material in the shocked region. The tongue immediately behind the head, which is also observed in the Mouse (Gaensler et al. 2004), represents the region where the particles are accelerated at the termination shock where the energy density of the pulsar wind is balanced by external pressure. The termination shock surface is elongated, having a significantly larger separation from the pulsar at the rear than in the direction of motion. As suggested in the simulations by Gaensler et al. (2004), the flow near the head of the bow shock advects the synchrotron-emitting particles back along the direction of motion of the pulsar, forming a broad cometary morphology as indicated by the radio plume. Material in this region generally moves supersonically. Directly behind the pulsar, material within the termination shock flows in a cylinder directed opposite to the pulsar’s velocity vector, forming a long narrow tail; the material in this region is subsonic. As also suggested by theoretical modeling, the broad tail region originates in the strongly shocked material located immediately behind the shock front. A narrow, collimated tail is produced by material flowing along the path of the running pulsar. This is indeed the morphology that has been observed in the case of the Mouse (Yusef-Zadeh & Bally 1987; Gaensler et al. 2004). Usually, the first shocked zone of the broad tail is highly magnetized while the narrow tail is more weakly magnetized (Bucciantini 2002; Romanova et al. 2005).

One of the noticeable differences in the radio structure between the Cannonball and the Mouse is the abrupt change from the broad radio plume to the narrow head-tongue structure, as observed in the radio images. The high-quality 2012 images of the Cannonball (Figure 3, for example) show this transition well. If the radio-emitting material is confined by a bow-shock, the shape of the radio structure would be characterized by a Mach cone with a Mach angle (μ); for a given Mach number M , $\sin \mu = 1/M$. For a smaller M , the shape of the bow-shock becomes blunter, *i.e.* a larger μ . The transition in the shape of the radio structure from the plume to the head might reflect

a significant change in Mach number of the Cannonball as the pulsar reaches the edge of the SNR; *i.e.* the Cannonball could become highly supersonic after departing from the SNR as the sound speed drops substantially in the ambient medium. Similar changes in PWN morphology were observed in the “Guitar” (Chatterjee & Cordes 2004); these authors argued that the morphology change reflects the random density inhomogeneities in the ISM; a high-density region in the Guitar path created the broad rounded end of the Guitar body.

Based on the radio images, the physical parameters can be calculated using the assumption that the source components are in equipartition by minimizing magnetic and synchrotron gas pressures. In the calculation, we assumed that both particle and magnetic-field filling factors are unity. The derived parameters are tabulated in Table 3. The pressures of the synchrotron-emitting gas of 0.7, 0.4 and 5×10^{-8} dyn cm⁻² are inferred for the compact head, the broad plume and the linear tail, respectively. The magnetic field strengths range from 0.2–0.3 mG for the head and broad plume to 0.8 mG for the long linear tail. The strength of the magnetic field inferred for the long narrow tail appears to be consistent with previous values inferred for the Galactic center region (Yusef-Zadeh & Morris 1987b; Morris & Yusef-Zadeh 1989; Morris 2007; Crocker et al. 2010). For a magnetic strength of 0.8 mG, the synchrotron cooling time is about 20,000 years.

4.2. Trajectory and bending

If the linear tail traces the trajectory of the Cannonball, then the Cannonball may have been launched at a position close to the geometric center of the Sgr A East SNR, as expected for a runaway neutron star created by a core collapse (Lai 2004), and it appears to have travelled along a straight line in PA=22° until it reached the boundary of the Sgr A East SNR where the emission cavity is located. Then, in this scenario, the direction of motion of the Cannonball appears to have changed before it departed from the cavity. The bending or the curvature of the Cannonball trajectory is the most remarkable feature that differs from the radio morphology of the Mouse. In the following analysis, we examine a possible explanation of the bending or curvature of the trajectory. First, if the curvature results from the gravity of the enclosed mass within the Cannonball orbit,

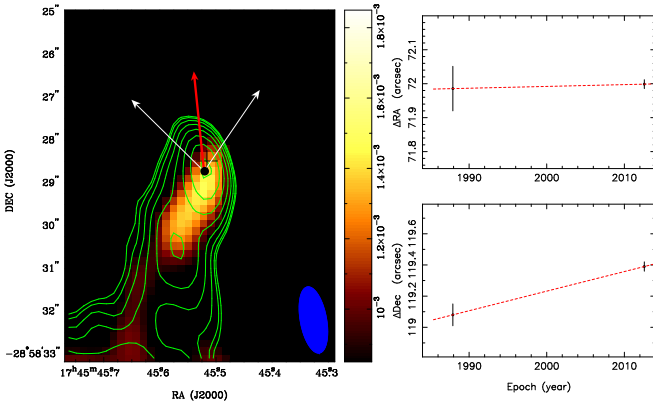


FIG. 4.— Left: The new VLA 5.5 GHz image (contours) observed in 2012 is overlaid on the archival 4.75 GHz image (color) observed in 1987 to show a positional displacement of the radio counterpart corresponding to the X-ray object, the Cannonball, between the two epochs. The contours are 0.12, 0.14, 0.16, 0.20, 0.32 mJy beam⁻¹. The black cross marks the Chandra position of the X-ray source determined from the ACIS-I observations in the period from March 29, 2000 to July 20, 2007 (Muno et al. 2009). The dot marks the VLA position of the peak emission at 5.5 GHz (2012). The red arrow anchored at the 5GHz peak indicates the proper motion vector ($\mu = 0.013$ arcsec yr⁻¹ or 500 km s⁻¹) in P.A. ($\Theta = 4^\circ$). The two white arrows indicate the $\pm 3\sigma$ uncertainty range of the P.A. ($\Delta\Theta_{3\sigma} = 40^\circ$). At the bottom-right is the FWHM beam. Right: The dashed lines show the motion implied by the two points separated in time along the horizontal axes. The vertical axis represents angular offsets from the common reference position. Error bars on the positions in each coordinate are $1-\sigma$.

the bending or deflection angle can be estimated. The total energy of the object per unit mass is given by,

$$E = \frac{1}{2}V^2 - \frac{GM}{R}, \quad (1)$$

where V is the velocity of the Cannonball, R is the distance of the Cannonball to the mass center and M is the enclosed mass within a radius of R . Given an enclosed mass of $M = 1.5 \times 10^7 M_\odot$ within a radius of 5 pc in the central region (Mezger, Duschl, & Zylka 1996; Genzel, Eisenhauer & Gillessen 2010; Do et al. 2013), the total energy would be positive for an object traveling with a velocity of > 162 km s⁻¹. The velocity of the Cannonball inferred from our proper motion measurements appears to be much greater than the escape velocity from this region, *i.e.* $E \approx \frac{1}{2}V^2$ for $V^2 \gg 2GM/R$. The Cannonball would then be on a hyperbolic orbit assuming Keplerian motion with respect to the center of the enclosed mass. Deviations due to gravitational interactions with other objects and an extended mass distribution were neglected in this approach. Then, the eccentricity³ of the Cannonball orbit is approximately,

$$e \approx \left[\frac{V}{30 \text{ km s}^{-1}} \right]^2 \left[\frac{R}{\text{AU}} \right] \left[\frac{M}{M_\odot} \right]^{-1}. \quad (2)$$

For the Cannonball, $e \approx 20$ is inferred using $R = 5.4$ pc and $M = 1.5 \times 10^7 M_\odot$.

The turning or bending angle is defined by the angle between the asymptotes of a hyperbolic orbit; for the Cannonball,

$$\psi = \arcsin\left(\frac{1}{e}\right) \approx \frac{1}{e} \sim 3^\circ, \quad (3)$$

which occurs when the object passes through periapse. The Cannonball appears to have moved farther away from the periapse if it was launched near the geometric center of the Sgr A East shell; we therefore conclude that the central enclosed mass makes an insignificant contribution to the curvature of the Cannonball's trajectory. The straight path of the Cannonball, if indicated by the linear tail, would be consistent with this picture.

A possible alternative explanation for the apparent change of direction (aside from the trivial case that the tail is a coincidentally superposed, unrelated phenomenon) is that the Cannonball has experienced an encounter with a massive stellar object (or multiple encounters with a group of stars) in the emission cavity. One critical problem in this explanation is that the probability of such a close encounter is very small, even for the high stellar density in the Galactic center region; for the mass of a typical star ($1 M_\odot$), a close encounter between the Cannonball star and a typical field star at $R_{\text{enc}} \approx 0.03$ AU is required to deflect the Cannonball trajectory by 25 degrees. The timescale for such an encounter can be estimated by $t_{\text{enc}} = (n\sigma v_{\text{disp}})^{-1} \approx 1 \times 10^{13}$ yr for stellar density $n \sim 3 \times 10^4$ pc⁻³, encounter cross section $\sigma \sim \pi R_{\text{enc}}^2 \sim 0.002$ AU², and for a stellar velocity dispersion in the central 5 pc of $v_{\text{disp}} \sim 50$ km s⁻¹ (Genzel, Eisenhauer & Gillessen 2010).

However, the probability of encounter would increase if the runaway pulsar had been born in a binary system, but still remained bound to its massive companion as it received an impulse in the supernova event (Manchester et al. 2006). With a binary semi-major axis a , the encounter distance $R_{\text{enc}} \approx a$. The encounter cross section increases considerably after taking into account the gravitational focussing of orbits (Leonard 1989). For a binary mass of $M_b = M_C + M_N$, the cross section of encountering an intruder mass of $M_i = 1 M_\odot$ is given by Moeckel & Bonnell (2013),

$$\sigma = \pi R_{\text{enc}}^2 \left(1 + \frac{2G(M_b + M_i)}{R_{\text{enc}} v_{\text{disp}}^2} \right). \quad (4)$$

For $M_C \sim 20 M_\odot$ – the mass of a high-mass companion such as that in J1740–3052 (Madsen et al. 2012), $M_N \sim 1.5 M_\odot$ – the mass of a neutron star and $R_{\text{enc}} \approx a \sim 10$ AU, the encounter cross section σ will increase by a factor of 3×10^6 as compared to that of the single pulsar system. Thus, the timescale for such an encounter is $\sim 5 \times 10^6$ yr. The probability of the observed deflection due to the gravitational bending in a binary encounter is greatly enhanced but is still very small compared to the pulsar lifetime, so this would have to be an unusually fortuitous occurrence. We therefore consider the scattering hypothesis to be unlikely, and do not discuss it further.

A third possibility is that, inside the Sgr A East SNR, the orientation of the tail is determined not only by the motion of the neutron star, but also by the lateral component of the orbital motion of the medium in which the tail is embedded: the SNR itself. Once the neutron star crossed the interface of the SNR with the local interstellar medium (ISM), the lateral motion of the medium surrounding it can differ substantially, and thereby make it appear as if the wake, or tail, has changed directions. In order to explain the 25 degree bend, given the pulsar velocity that we infer, the lateral velocity difference between the two media would need to be about 200 km s⁻¹, which is somewhat larger than the circular orbital velocity of 35 km s⁻¹ in this region, presenting a difficult, though perhaps not impossible, challenge for this hypothesis.

³ see <http://www.braeunig.us/space/orbmech.htm>

An alternative explanation may be that the head-tongue association is unrelated to the plume-tail structure. In this case, the observed proper motion of the neutron star is consistent with originating at the center of Sgr A East without any deflection. That the head-tongue association does not point back toward the center of Sgr A East can be explained by some combination of the bulk orbital motion of the SNR since its formation, and the differential velocity of the medium surrounding the SNR shell relative to the shell itself.

4.3. Age of the object

The distance between the Cannonball and the estimated geometrical center of the Sgr A East SNR is ~ 4.7 pc ($120''$), assuming that the Sgr A East SNR is located at the same distance of 8 kpc as that of Sgr A* (Reid et al. 2009). Given the ~ 500 km s $^{-1}$ lateral velocity of the Cannonball, the time required for traveling from the center of the SNR to its present position is 9000 years, neglecting any effect of deceleration or acceleration. If the Cannonball is a runaway neutron star from the core-collapse SN explosion, the age of Sgr A East is the same. This agrees well with the SNR expansion age proposed by Mezger et al. (1989). The time for a pulsar crossing the SNR to move into the ambient ISM is given by van der Swaluw et al. (2003) as,

$$t_{\text{cross}} = 44 \times 10^3 \text{ y} \left[\frac{E_{\text{SN}}}{10^{51} \text{ erg}} \right]^{1/3} \left[\frac{n_0}{1 \text{ cm}^{-3}} \right]^{-1/3} \left[\frac{V_{\text{PSR}}}{500 \text{ km s}^{-1}} \right]. \quad (5)$$

For a typical pulsar in the galactic plane, the crossing time is ~ 44000 yr. For the Galactic center environment, with a higher density (n_0) of the ambient medium (Mezger et al. 1989), a shorter crossing time is expected, consistent with our 9000 year estimate if the ambient density is about 100 cm $^{-3}$.

5. CONCLUSION

The radio counterpart of the X-ray Cannonball was detected in our VLA observations in 2012 at 5.5 GHz as well as in archival data from 1987 at 4.75 GHz and in the period between 1990 and 2002 at 8.31 GHz. Based on the observed morphology and our analysis, the radio source can be characterized as a compact head with a trailing “tongue”, possibly connecting to a broad radio plume followed by a linear tail. Such a morphol-

ogy appears to be common for PWNe powered by a runaway pulsar. The inferred total radio luminosity of $\sim 8 \times 10^{33}$ erg s $^{-1}$ is consistent with the hypothesis that the emitting relativistic electrons in the radio source are supplied via the pulsar wind powered by a neutron star produced in the SN explosion that created the Sgr A East SNR. The inferred proper motion implies a transverse velocity of 500 ± 100 km s $^{-1}$. If the Cannonball is associated with the Sgr A East SNR, an age of ~ 9000 year is inferred for both objects.

We thank Sangwook Park for providing us his three-color X-ray image. We are grateful to R. V. Urvashi and the CASA staff for assistance with the data reduction. We are grateful to the referee for his/her valuable comments and suggestions. The Jansky Very Large Array (VLA) is operated by the National Radio Astronomy Observatory (NRAO). The NRAO is a facility of the National Science Foundation operated under cooperative agreement by Associated Universities, Inc. The research has made use of NASA’s Astrophysics Data System.

REFERENCES

- Bevington, P. R. & Robinson, D. K. 2002, *Data Reduction and Error Analysis for the Physical Sciences*, McGraw-Hill, New York
- Bucciantini, N. 2002, AA, 387, 1066
- Chatterjee, S., & Cordes, J. M. 2002, ApJ, 575, 407
- Chatterjee, S., & Cordes, J. M. 2004, ApJ, 600, L51
- Crocker, R. M., Jones, D. I., Melia, F., Ott, J. & Protheroe, R. J. 2010, Nature, 463, 65
- Do, T., Lu, J. R., Ghez, A. M., Morris, M. R., Yelda, S., Martinez, G. D., Wright, S. A., & Matthews, K. 2013, ApJ764, 154
- Gaensler, B. M., van der Swaluw, E., Camilo, F., Kaspi, V. M., Baganoff, F. K., Yusef-Zadeh, F., & Manchester, R. N. 2004, ApJ, 616, 383
- Gaensler, B. M. & Slane, P. O. 2006, ARA&A
- Gaensler, B. M., Chatterjee S., Slane, P. O., van der Swaluw, E., Camilo F., & Hughes, J. P. 2006, ApJ, 648, 1037
- Genzel, R., Eisenhauer, F., & Gillessen, S. 2010, Rev. Mod. Phys., 82, 3121
- Goss, W. M., Schwarz, U. J., van Gorkom, J. H. & Ekers, R. D. 1985, MNRAS, 215, 69
- Green, D. A. 1984, MNRAS, 209, 449
- Jones, T. W., 1974, AA, 30, 37
- Khokhlov & Melia, F. 1996, ApJ, 457, L61
- Lai, D., 2004, in *Cosmic Explosions in Three Dimensions: Asymmetries in Supernovae and Gamma-Ray Bursts*, ed. P. Höflich, P. Kumar, J. C. Wheeler, UK: Cambridge University Press, p.276
- Lee, S., Pak, S., Lee, S.-G., Geballe, T. R., Choi, M., Davis, C. J., Herrmstein, R. M., & Minh, Y. C. 2007, ASP Conference Series, Vol. 362, 158
- Leonard P. J. T., 1989, AJ, 98, 217
- Madsen, E. C., Stairs, I. H., Kramer, M., Camilo, F., Hobbs, G. B., Janssen, G. H., Lyne, A. G., Manchester, R. N., Possenti, A. & Stappers, B. W. 2012, MNRAS, 425, 2378
- Maeda, Y., Baganoff, F. K., Feigelson, E. D., Morris, M., Bautz, M. W., Brandt, W. N., Burrows, D. N., Doty, J. P., Garmire, G. P., Pravdo, S. H., Ricker, G. R., Townsley, L. K. 2002, ApJ, 570, 671
- Manchester, R. N. 2006, AdSpR, 38, 2709
- Mezger, P. G., Zylka, R., Salter, C. J., Wink, J. E., Chini, R., Kreysa, E., & Tuffs, R. 1989, AA, 209, 337
- Mezger, P. G., Duschl, W. J., & Zylka, R. 1996, AAR, 7, 289
- Moeckel, N. & Bonnell, I. A. 2013, arXiv:1301.6959v1, eprint
- Morris, M. & Yusef-Zadeh, F. 1989, ApJ, 343, 703
- Morris, M. 2007, J. Phys.: Conf. Ser. 54, eds: R. Schödel, G.C. Bower, M.P. Muno, S. Nayakshin & T. Ott, pp. 1-9 (2006) astro-ph/0701050
- Morris, M. R., Zhao, J.-H. & Goss, W. M. 2013, ApJ, in preparation
- Muno, M. P., Baganoff, F. K., Bautz, M. W., Brandt, W. N., Broos, P. S., Feigelson, E. D., Garmire, G. P. Morris, M., Ricker, G. R. Townsley, L. K. 2003, ApJ, 589, 225
- Muno, M. P., Bauer, F. E., Baganoff, F. K., et al. 2009, ApJS, 181, 110
- Park, S., Muno, M. P., Baganoff, F. K., Maeda, Y., Morris, M., Chartas, G., Sanwal D., Burrows D. N., Garmire, G. P. 2005, ApJ, 631, 963
- Pedlar, A., Anantharamaiah, K.R., Ekers, R. D., Goss, W. M., van Gorkom, J. H., Schwarz, U. J., & Zhao, J.-H. 1989, ApJ, 342, 769
- Reid, M. J. & Brunthaler, A. 2004, ApJ, 616, 872
- Reid, M. J., Reid, M. J., Menten, K. M., Zheng, X. W., Brunthaler, A., Moscadelli, L., Xu, Y., Zhang, B., Sato, M., Honma, M., Hirota, T., Hachisuka, K., Choi, Y. K., Moellenbrock, G. A., Bartkiewicz, A. 2009, ApJ, 700, 137

TABLE 3

PHYSICAL CONDITIONS OF THE RADIO SOURCE ASSOCIATED WITH THE CANNONBALL

Parameters	Head	Plume	Linear tail
size (pc)	0.08×0.04	1.2×0.6	1.2×0.08
L_R (10^{33} erg s $^{-1}$)	0.01	5	3.0
B_{min} (mG)	0.3	0.2	0.8
P_{min} (10^{-8} dyn cm $^{-2}$)	0.7	0.4	5
t_{syn} (10^5 yr)	1	2	0.2

Row 1: the linear size;

Row 2: radio luminosity in 0.1 GHz $< \nu < 100$ GHz;

Row 3: minimum magnetic field strength;

Row 4: minimum pressure of particles;

Row 5: synchrotron cooling time.

- Rockefeller, G., Fryer, C. L., Baganoff, F. K. & Melia, F. 2005, *ApJL*, 635, L141
- Romanova, M. M., Chulsky, G. A., & Lovelace, R. V. E. 2005, *ApJ*, 630, 1020
- van der Swaluw, E., Achterberg, A., Gallant, Y. A., Downes, T. P., Keppens, R. 2003, *AA*, 397, 913
- Woltjer L., Salvati, M., Pacini, F., & Bandiera, R. 1997, *AA*, 325, 295
- Yusef-Zadeh, F. & Morris, M. 1987, *ApJ*, 320, 545
- Yusef-Zadeh, F. & Morris, M. 1987, *AJ*, 94, 1178
- Yusef-Zadeh, F. & Bally, J. 1987, *Nature*, 330, 455
- Zeiger, B. R., Briskin, W. F., Chatterjee, S. & Goss, W. M. 2008, *ApJ*, 674, 27
- Zhao, J.-H., Morris, M. R., Goss, W. M. & An, T. 2009, *ApJ*, 699, 186
- Zhao, J.-H., Morris, M. R., & Goss, W. M. 2013, *ApJ*, in preparation